Pulsed electrodeposition of single-crystalline Bi_2Te_3 nanowire arrays

2006 Nanotechnology 17 1706

(http://iopscience.iop.org/0957-4484/17/6/027)

INSTITUTE OF PHYSICS PUBLISHING NANOTECHNOLOGY
Nanotechnology **17** (2006) 1706–1712 doi:10.1088/0957-4484/17/6/027

Pulsed electrodeposition of single-crystalline Bi_2Te_3 nanowire arrays

Liang Li, Youwen Yang, Xiaohu Huang, Guanghai Li[1] and Lide Zhang

Key Laboratory of Materials Physics, Anhui Key Laboratory of Nanomaterials and Nanotechnology, Institute of Solid State Physics, Chinese Academy of Sciences, Hefei 230031, People's Republic of China

E-mail: ghli@issp.ac.cn

Received 27 September 2005
Published 27 February 2006
Online at stacks.iop.org/Nano/17/1706

Abstract
Thermoelectric material Bi_2Te_3 nanowire arrays have been successfully prepared by pulsed electrochemical deposition into the nanochannels of porous anodic alumina membranes. X-ray diffraction analyses show that the as-synthesized nanowires have a highly preferential orientation. Scanning electron microscopy, transmission electron microscopy, and high-resolution transmission electron microscopy observations indicate that the high-filling-rate and uniform Bi_2Te_3 nanowires are single crystalline. Energy dispersive spectrometer analyses indicate that the compositions of the nanowires can be controlled by changing the potentials and the solution concentrations. The electrical resistance measurements indicate that the resistances increase with decreasing temperature and show a typical semiconductor characteristic. The growth mechanism is discussed together with the electrochemical deposition process studies.

1. Introduction

There is a growing interest in low-dimensional thermoelectric (TE) materials because of the theoretical prediction that quantum confinement will increase the TE efficiencies of materials compared with bulk [1, 2]. A single nanowire cannot carry a high enough current for TE applications, thus the synthetic methods that yield high-quality nanowire arrays are of particular interest [3]. Many types of TE material nanowire arrays, such as Bi, Sb, $Bi_{1-x}Sb_x$, $Bi_{2-x}Sb_xTe_3$, and $Bi_2Te_{3-y}Se_y$ [4–11], have been fabricated by different techniques in the anodic alumina membranes (AAMs) with uniformly sized, high-density and high-aspect-ratio nanochannels [12–18].

Bismuth telluride (Bi_2Te_3) and its solid solutions are well known good TE materials for near-room-temperature applications. Bulk Bi_2Te_3 has a good TE figure of merit and has been widely used in commercial applications. Theoretical studies suggest that one-dimensional Bi_2Te_3 nanowires may have a higher figure of merit than that of bulk materials, which have stimulated study in the fabrication of Bi_2Te_3 nanowire arrays [19, 20]. Recently, Bi_2Te_3 nanowire arrays have been fabricated by direct-current electrochemical deposition in the AAM [21–24]. It is still a challenge, however, to fabricate high-filling, high-aspect-ratio, large-area, uniform, and high-quality single-crystalline nanowire arrays. Moreover, detailed study on the growth process of the Bi_2Te_3 nanowire arrays is still scarce. The electrical resistance properties of Bi_2Te_3 bulk materials and thin films near room temperature have been systematically studied, but little attention has been paid to one-dimensional Bi_2Te_3 nanowires, which might also be due to the difficulty of the direct fabrication of high-quality single-crystalline Bi_2Te_3 nanowire arrays.

In this paper, we report the fabrication and electrical transport property of high-filling-rate, highly oriented, and single-crystalline Bi_2Te_3 nanowire arrays in the nanochannels of AAM by the pulsed electrochemical deposition for the first time. The growth mechanism and the electrochemical deposition process of the nanowires are discussed in detail.

2. Experimental procedures

The AAM was prepared using a two-step anodic anodization process as described previously [25–29]. The AAMs with

[1] Author to whom any correspondence should be addressed.

the pore sizes of about 40 and 60 nm were used. A layer of Au film (thickness 200 nm) was sputtered onto one side of the AAM to serve as the working electrode in a common two-electrode plating cell, and a graphite plate was used as the counter-electrode. Bi_2Te_3 nanowire arrays were deposited under modulated voltage control and a potential of −1.3 V was applied between the two electrodes. During the pulse time, 3 ms, metal species were electrochemically reduced on the pore ground of the AAM. The delayed time, 10 ms, provided time for the recovery of the ion concentration [7, 30]. The electrolyte was prepared by dissolving 0.01 M $Bi(NO_3)_3{\cdot}5H_2O$ and 0.015 M TeO_2 in HNO_3 solution. The pH of the final electrolyte was adjusted to about 1 with HNO_3.

X-ray diffractometry (XRD, Philips PW 1700× with Cu Kα radiation), field-emission scanning electron microscopy (FE-SEM, FEI Sirion-200), transmission electron microscopy (TEM, H-800), selected area electron diffraction (SAED), and high-resolution transmission electron microscopy (HRTEM, JEOL-2010) were used to study the crystalline structure and morphology of nanowire arrays. The chemical compositions of the nanowires were determined by an energy dispersive spectrometer (EDS) attached to the SEM. The electrical resistance was measured on a physical property measurement system (PPMS) designed by American Quantum Design Company. The overfilled particles on the surface of the AAM were mechanically polished away with Al_2O_3 nanopowders for XRD measurements. For SEM observations, the AAM was partly dissolved with 0.5 M NaOH solution, and then carefully rinsed with deionized water several times. For TEM and HRTEM observations, the AAM was completely dissolved with 1 M NaOH solution and then rinsed with absolute ethanol. A drop of solution was placed on a carbon grid and allowed to dry prior to electron microscopy analysis.

3. Results and discussion

Figure 1(a) shows the XRD pattern of the Bi_2Te_3 nanowire array fabricated by pulsed electrodeposition (sample I). Only (015) and (0210) peaks of the hexagonal Bi_2Te_3 (JCPDS No 72-2036) can be seen, and the ratio of these two indices is an integer, indicating that the Bi_2Te_3 nanowires have a highly preferential orientation along the [015] direction, which will be further confirmed by HRTEM observation. No other diffraction peaks, such as the elemental Bi and Te, can be detected, indicating the nanowires are a pure Bi_2Te_3 phase. As comparison, figure 1(b) shows the XRD pattern of the Bi_2Te_3 nanowire array fabricated by direct-current electrodeposition (sample II). There are predominant (015) and (0210) peaks together with a small peak corresponding to the (110) plane, which indicates that this sample has no complete preferred orientation.

Harris texture analysis was used to quantify the orientation in the nanowires [31, 32]. The texture coefficient, which gives the measurement of the orientation of each reflection compared to a completely randomly oriented sample, is expressed as follows:

$$C_{(hkl)} = \frac{\frac{I_{(hkl)}}{I_{o(hkl)}}}{N^{-1}\sum_N \left(\frac{I_{(hkl)}}{I_{o(hkl)}}\right)}, \qquad (1)$$

where $C_{(hkl)}$ is the texture coefficient of the (hkl) plane, $I_{(hkl)}$ is the measured relative intensity of the (hkl) plane, $I_{o(hkl)}$ is the relative intensity of the corresponding plane given in the JCPDS data file and N is the number of reflections considered in the analysis. It is clear from the definitions that the value of $C_{(hkl)}$ for the peak under investigation ranges from unity for a randomly oriented sample to N for a sample having a complete preferential orientation. The value of $C_{(hkl)}$ indicates the maximum preferred orientation of the nanowire arrays along the corresponding plane. The preferred orientation of each sample as a whole was analysed from the standard deviation (σ) of the texture coefficient ($C_{(hkl)}$),

$$\sigma = \sqrt{\frac{\sum_N (C_{(hkl)} - 1)^2}{N}} \qquad (2)$$

and an increase in the standard deviation is an indication of the orientation towards a particular plane for which the texture coefficient has a higher value.

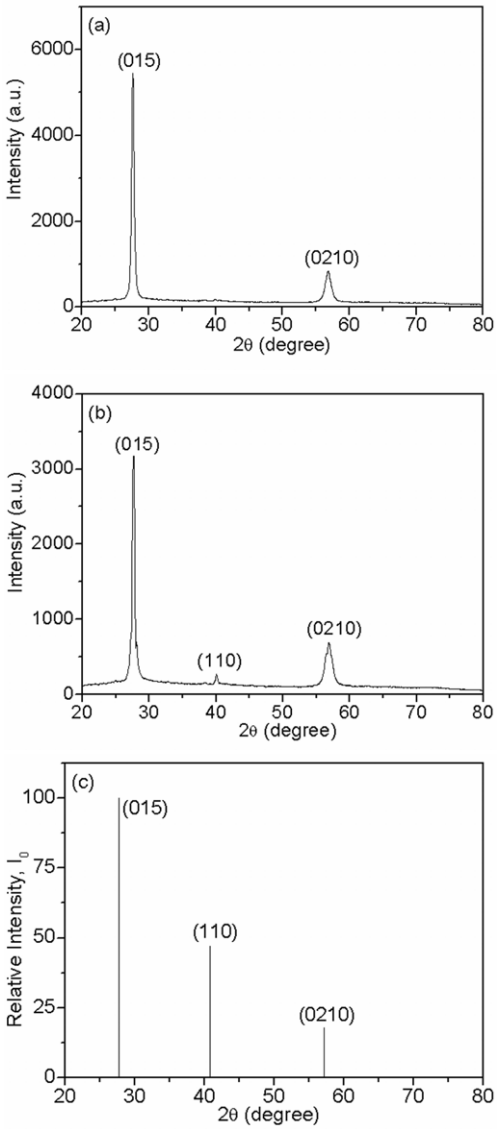

Figure 1. X-ray diffraction pattern of the Bi_2Te_3 nanowire array with the diameter of 40 nm fabricated by (a) pulsed electrodeposition and (b) direct-current deposition. (c) Bi_2Te_3—JCPDS pattern.

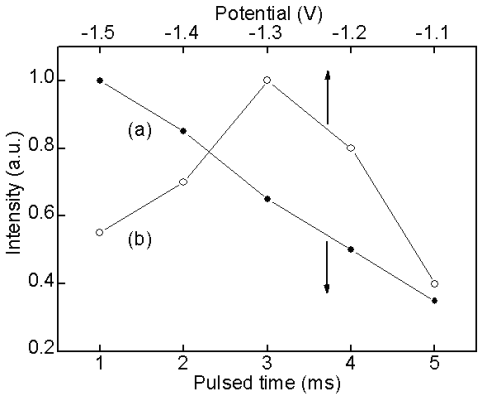

Figure 2. Relative intensity of (015) peak of Bi_2Te_3 nanowires as a function of (a) pulse time and (b) potential.

The values of $C_{(hkl)}$ and σ obtained for the Bi_2Te_3 nanowire arrays fabricated respectively by the direct-current and the pulsed electrodeposition are given in table 1. From this table one can see that (i) for (015) and (0210) planes the values of $C_{(hkl)}$ for sample I are much larger than unity and close to two (N), and those for sample II are much smaller than three (N) although larger than unity, and (ii) the value of σ for sample I is larger than that for sample II. From this analysis we can thus conclude that sample I has a highly preferential orientation along the [015] direction compared with sample II, and the pulsed electrodeposition technique provides a more effective method to fabricate highly oriented Bi_2Te_3 nanowire arrays.

To determine the optimal parameters for fabricating highly oriented and single-crystalline Bi_2Te_3 nanowire arrays, two series of experiments were respectively conducted under the conditions of the different potentials at a fixed pulse time and different pulse times at a fixed potential. Figure 2 shows the dependence of the (015) peak intensity of XRD patterns of the Bi_2Te_3 nanowires on the potential and pulse time. One can see that the peak intensity firstly increases, after reaching a maximum value at the potential of -1.3 V, and then decreases with further increasing the potential. The reduction in the peak intensity might be due to the hydrogen evolution at high potentials, which suppresses the growth of the nanowires along the (015) orientation. Therefore, the highly oriented Bi_2Te_3 nanowire arrays could be fabricated at the potential of about -1.3 V. Keeping the delayed time at a constant 10 ms, the (015) peak intensity always decreases with increasing pulse time. From this result we appear to conclude that the most appropriate pulse time is about 1 ms, but the corresponding potential is high (about -1.5 V), which leads to hydrogen evolution and an increase in the deposition rate, and thus the formed nanowires have a poor crystallinity. From the above analyses, we therefore select the potential of about -1.3 V and the pulse time of about 3 ms to fabricate highly oriented nanowire arrays.

The SEM images of the Bi_2Te_3 nanowire array after etching in 0.5 M NaOH solution for different times are shown in figure 3. Figure 3(a) is the bottom surface image of the nanowire array after mechanically polishing with Al_2O_3 nanopowders and then etching for 2 min. The result shown

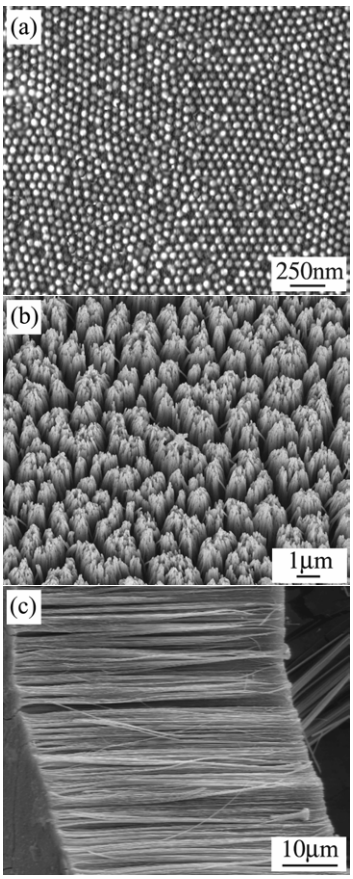

Figure 3. SEM images of the Bi_2Te_3 nanowire array with the diameter of 40 nm: (a) bottom view, (b) surface view and (c) cross-sectional view after etching for 2, 8 and 15 min, respectively.

in figure 3(a) is ubiquitous, and when the SEM probe moved to the different areas on the sample surface, the same image was always observed. This result clearly indicates that the nanowire array has a high filling rate. Figure 3(b) shows the surface image of the nanowire arrays after etching for 8 min; it shows that all the nanowires have the same height, implying that the pulsed electrodeposition is a well controlled process and all the nanowires are deposited along the pores at the same rate. Figure 3(c) shows the cross-sectional image of the nanowire array after etching 15 min. The length of the nanowires is about 50 μm, corresponding to the thickness of the AAM used.

Figure 4(a) shows a typical TEM image of the Bi_2Te_3 nanowire completely removed from the AAM. It is obvious that the Bi_2Te_3 nanowires have a smooth surface and a high aspect ratio. The diameter of the nanowire is uniform and equal to the pore size (40 nm) of the AAM used. In order to convincingly demonstrate the crystalline status of the nanowire, the SAED patterns were taken along the nanowire, and the results show that the diffraction patterns do not change along the nanowire except for a slight variation in the intensity of the individual spots, indicating that there is a slight structural deformation, which might result from the mechanical force during the ultrasonication treatment of the TEM samples. The same phenomenon was also commonly observed in other nanosystems [33, 34]. To investigate the

Table 1. Harris texture analysis of Bi_2Te_3 nanowire arrays.

Sample	Peak (*hkl*)	Intensity, $I_{(hkl)}$ (experiment)	Intensity, $I_{o(hkl)}$ (JCPDS)	Texture coefficient, $C_{(hkl)}$	Standard deviation, σ
I	015	100	100	1.7045	0.5450
	0210	13.66	18	1.2955	
II	015	100	100	1.2658	0.5372
	110	9.23	47	0.2532	
	0210	21.13	18	1.4810	

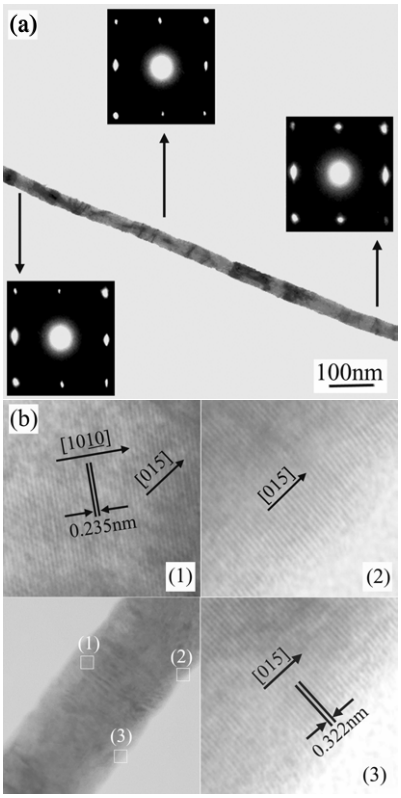

Figure 4. (a) TEM image and SAED patterns of a randomly selected single Bi_2Te_3 nanowire with the diameter of 40 nm. (b) Corresponding HRTEM images: (1), (2) and (3) are the magnified HRTEM images in the areas marked by three squares.

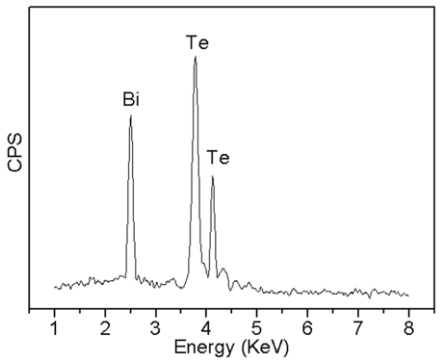

Figure 5. EDS pattern of the Bi_2Te_3 nanowires.

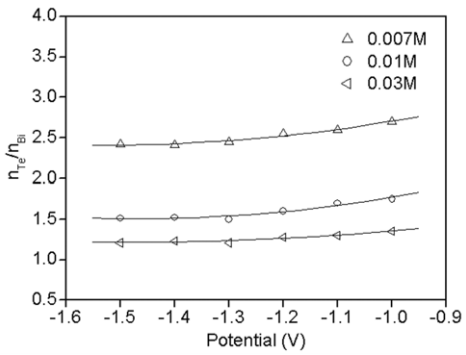

Figure 6. Dependence of the atomic ratio of Te to Bi in the Bi–Te nanowires on the potential from solutions containing 0.015 M TeO_2 and different Bi concentrations.

microstructure of nanowires we randomly selected a nanowire, and the corresponding HRTEM image is shown in figure 4(b). The clear lattice fringes with an identical orientation in three different regions marked by the white squares demonstrated that the nanowire has a uniform structure and is a single crystal with a preferential growth along the [015] direction. To estimate the crystalline status of all the nanowires in a textured sample, as commonly done in references [35, 36], we randomly selected some nanowires under HRTEM and statistical results indicated that about 90% of the nanowires had the preferred [015] direction, in agreement with the XRD results.

The composition of Bi_2Te_3 nanowires is shown in figure 5, which verifies that the nanowires consist of only Bi and Te. The quantitative analysis indicates that the atomic ratio of Bi to Te is close to 2:3. The stoichiometric (2:3) Bi–Te nanowires can be obtained by choosing the suitable potentials and the relative concentrations of Bi and Te in the electrolytes. Figure 6 shows the potential dependence of the compositions of the Bi–Te nanowires fabricated from the electrolytes with different Bi concentrations. It is noticed that (i) the atomic ratio of Te/Bi in the nanowires has the same changing trend with potential for various Bi concentrations, which decreases up to a certain potential and then reaches a constant value as the potential becomes more negative, and (ii) the nanowires deposited from the solution containing 0.01 M Bi have stoichiometric compositions at more negative potentials ($\leqslant -1.3$ V). High potentials may cause hydrogen evolution and greatly increase the deposition rate, and therefore the lower potential of -1.3 V is chosen in our experiment.

The electrochemical deposition process of the Bi_2Te_3 nanowires basically involves three steps [37, 38]:

(i) The diffusion and the absorption of Bi^{3+} and $HTeO_2^+$ ions to the Au electrode surface by the electric field force applied between two electrodes.

(ii) The reduction of the absorbed Bi^{3+} and $HTeO_2^+$ ions at the cathode by the chemical reactions

$$Bi^{3+} + 3e^- = Bi(s) \quad (3)$$

$$HTeO_2^+ + 3H^+ + 4e^- = Te(s) + 2H_2O. \quad (4)$$

(iii) The reduced Bi and Te react to form Bi_2Te_3.

Therefore, the overall chemical reaction can be expressed as

$$3HTeO_2^+ + 9H^+ + 18e^- + 2Bi^{3+} = Bi_2Te_3(s) + 6H_2O. \quad (5)$$

Step (i) is a rate-controlled process, which is determined by the current density or potential. Step (ii) occurs at a faster rate than step (i). These two steps determine the composition of the nanowires. Step (iii) mainly affects the crystalline nature of the nanowire.

To synthesize high-filling-rate, highly oriented and single-crystalline Bi_2Te_3 nanowire arrays by the electrochemical deposition in the AAM, several factors should be considered. Firstly, to avoid excessive cracking in the AAM while maintaining structural integrity, the AAM should have a large thickness, because the deposition will occur predominantly in the cracks due to greater accessibility of cations. Secondly, the AAM should be sonicated in water for a few minutes to remove the impurities and air bubbles in the nanopores of the AAM before electrodeposition, because the ions will preferentially nucleate and grow at the impurities, causing the inhomogeneous growth of nanowires, and the air bubbles will hinder the ion diffusion into the nanopores of the AAM, causing the electrodeposition on the surface of the AAM. Thirdly, to obtain dense, highly oriented and single-crystalline Bi_2Te_3 nanowires, the control of the growth rate is critical. Three measures can be used: (i) reducing the concentrations of Bi and Te to about 1×10^{-2} M (until the limit where H_2 begins to be produced); (ii) lowering the temperature to about 1 °C; (iii) employing the pulsed electrodeposition technique, which allows a better control over the deposition rate and ion concentration at the deposition interface, as compared with the direct and alternating current deposition [39, 40]. In the present study, the pulse time (3 ms) was so short that only a small number of metal ions at the interfaces are consumed. The delay time (10 ms) provided enough time for the concentration of the metal ions at the pore tips to achieve a steady state through diffusion. No evident concentration gradient near the reaction interface exists during the deposition, and the pulse time controls the atom-by-atom deposition of nanowires, which increases the crystallinity and compositional homogeneity of the nanowires [11].

Figure 7 shows the variation of electrical resistance as a function of temperature for the Bi_2Te_3 nanowires with the diameter of 40 nm (figure 7(a)) and 60 nm (figure 7(b)). Because Bi_2Te_3 and its solid solutions are currently the leading thermoelectric materials for near-room-temperature cooling applications, only the electrical resistances near room temperature are given here. One can see that the electrical resistances decrease with temperature, and exhibit a negative temperature coefficient of resistance (TCR), i.e. a typical semiconductor-like character. From figure 7 one can obtain the TCRs of the Bi_2Te_3 nanowires, which are about -1.25×10^{-4} and -2.16×10^{-3} K^{-1} for 40 and 60 nm nanowires respectively. The TCR of the 40 nm nanowires is much smaller than that of 60 nm nanowires, indicating that the nanowires with smaller diameter have lower resistance sensitivity to temperature. The near linearity of the dependence of InR on $1/T$ shown in the insets in figure 7 further proves that the Bi_2Te_3 nanowires with the diameters of 40 and 60 nm all exhibit the normal semiconducting behaviour.

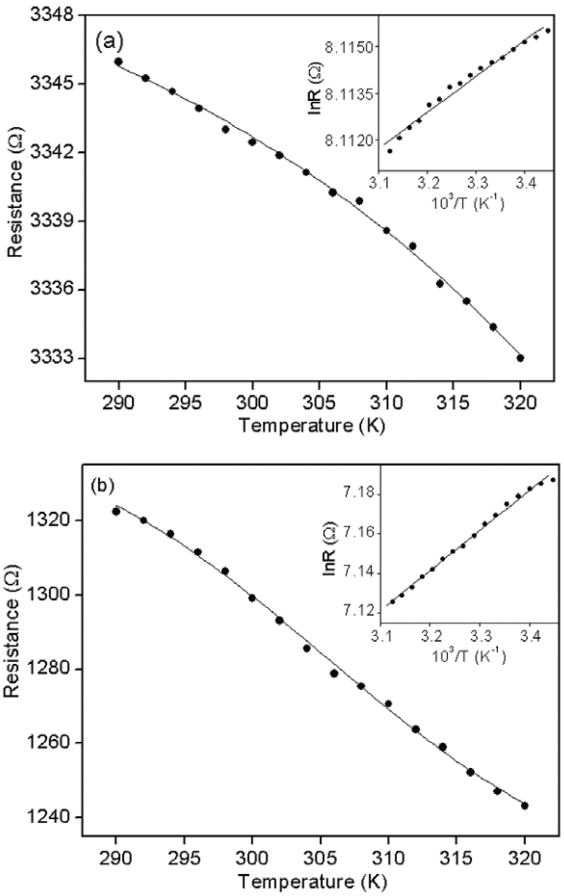

Figure 7. Temperature dependence of the electrical resistance for the Bi_2Te_3 nanowires with different diameters: (a) 40 nm and (b) 60 nm. The insets are the plots of ln R versus $1/T$.

Due to the limitations imposed by the sample geometry, a two-probe measurement was conducted by bringing two copper wires with silver epoxy to a small area (typically 1–2 mm^2) on both sides of the AAM. Since the silver particle size in the silver paint is of the order of 1 μm, the silver paint may only make good contact to a small fraction of the total number of wires of the sample. Therefore, we could not estimate the total number of wires connected to the two electrical contacts, and the actual resistivity value of the nanowires is unknown, as generally shown in the literature [5, 41].

Bismuth telluride belongs to the crystal class of $R\bar{3}m$ and therefore possesses the associated anisotropy of transport properties, such as the electrical resistance, thermoelectricity, etc. For Bi_2Te_3 bulk material and thin film, three discrepant temperature dependences of the electrical resistance have been obtained: (i) a gradual increase with rising

temperature; (ii) an initial increase and then decrease with temperature; (iii) a gradual decrease with increasing temperature. The observed discrepancy of the temperature dependence of the electrical resistance might be attributed to the different preparation conditions, which leads to the different compositions and defects, and poly- or single-crystalline structure [42–45]. For polycrystalline Bi_2Te_3 nanowires, theoretical calculation indicated that the resistance increases with increasing temperature in the framework of the relaxation time approximation, i.e., a metal-like character [46]. For Bi_2Te_3 single-crystalline nanowires, the scattering processes of the carriers are expected to be different from those in the polycrystalline state, and both the carrier mobility and the carrier density affect the character of the temperature-dependent electrical resistance. The increased carrier concentrations and decreased carrier mobility with increasing temperature play a dominant role in determining the temperature behaviour of the electrical resistance. The surface and wire boundary scatterings should also be taken into account along with the defect scattering and electron–phonon scattering [47]. The lower resistance sensitivity to temperature of the Bi_2Te_3 nanowires with smaller diameter could make them better candidates for TE application near room temperature [48], and further study is underway.

4. Conclusions

In summary, high-filling-rate, highly oriented, and ordered Bi_2Te_3 nanowire arrays have been fabricated from aqueous solution by pulsed electrochemical deposition into the pores of AAM. The Bi_2Te_3 nanowires are single crystalline and have a preferential orientation along the [015] direction. It was found that the optimum growth condition could be achieved by the proper choice of the pulsed parameters and the deposition potentials and ion concentrations in the electrolyte. The electrical transport measurements show that the Bi_2Te_3 nanowires with the diameters of 40 and 60 nm all exhibit a typical semiconductor behaviour, and the 40 nm nanowire has lower resistance sensitivity to temperature than the 60 nm nanowire. We believe that the detailed study will help in fabricating other single-crystalline nanowire arrays, and the Bi_2Te_3 single-crystalline nanowire arrays will find potential applications in thermoelectric nanodevices in the future.

Acknowledgments

This work was supported by the National Natural Science Foundation of China (No. 10474098) and the National Major Project of Fundamental Research for Nanomaterials and Nanostructures (No. 2005CB623603).

References

[1] Hicks L D and Dresselhaus M S 1993 *Phys. Rev.* B **63** 3230
[2] Hicks L D, Harman T C, Sun X and Dresselhaus M S 1996 *Phys. Rev.* B **53** 10493
[3] Prieto A L, Martín-González M, Keyani J, Gronsky R, Sands T and Stacy A M 2003 *J. Am. Chem. Soc.* **15** 2388
[4] Zhang Z B, Gekhtman D, Dresselhaus M S and Ying J Y 1999 *Chem. Mater.* **1** 1659
[5] Heremans J, Thrush C M, Lin Y M, Zhang Z, Dresselhauls M S and Mansfield J F 2000 *Phys. Rev.* B **61** 2921
[6] Huber T E, Celestine K and Graf M 2003 *Phys. Rev.* B **67** 245317
[7] Zhang Y, Li G H, Wu Y C, Zhang B, Song W H and Zhang L D 2002 *Adv. Mater.* **14** 1227
[8] Peng Y, Qin D H, Zhou R J and Li H L 2000 *Mater. Sci. Eng.* B **77** 246
[9] Martín-González M, Prieto A L, Gronsky R, Sands T and Stacy A M 2003 *Adv. Mater.* **15** 1003
[10] Martín-González M, Snyder G J, Prieto A L, Gronsky R, Sands T and Stacy A M 2003 *Nano Lett.* **3** 973
[11] Li L, Li G H, Zhang Y, Yang Y W and Zhang L D 2004 *J. Phys. Chem.* B **108** 19380
[12] Guo Y G, Hu J S, Liang H P, Wan L J and Bai C L 2005 *Adv. Funct. Mater.* **15** 196
[13] Sklar G P, Paramguru K, Misra M and LaCombe J C 2005 *Nanotechnology* **16** 1265
[14] Wu G S, Zhang L D, Cheng B C, Xie T and Yuan X Y 2004 *J. Am. Chem. Soc.* **126** 5976
[15] Pan H, Sun H, Poh C, Feng Y P and Lin J Y 2005 *Nanotechnology* **16** 1559
[16] Xu D S, Shi X S, Guo G L, Gui L L and Tang Y Q 2000 *J. Phys. Chem.* B **104** 5061
[17] Shen X P, Yuan A H, Hu Y M, Jiang Y, Xu Z and Hu Z 2005 *Nanotechnology* **16** 2039
[18] Choi J, Sauer G, Nielsch K, Wehrspohn R B and Gösele U 2003 *Chem. Mater.* **15** 776
[19] Venkatasubramanian R, Siivola E, Colpitts T and O'Quinn B 2001 *Nature* **413** 597
[20] Sander M S, Cote M J, Gu W, Kile B M and Tripp C P 2000 *Adv. Mater.* **12** 520
[21] Sander M S, Gronsky R, Sands T and Stacy A M 2003 *Chem. Mater.* **15** 335
[22] Sander M S, Prieto A L, Gronsky R, Sands T and Stacy A M 2002 *Adv. Mater.* **14** 665
[23] Prieto A L, Sander M S, Martín-González M, Gronsky R, Sands T and Stacy A M 2001 *J. Am. Chem. Soc.* **123** 7160
[24] Sapp S A, Lakshmi B B and Martin C R 1999 *Adv. Mater.* **11** 402
[25] Jin C G, Zhang G Q, Qian T, Li X G and Yao Z 2004 *J. Phys. Chem.* B **108** 1844
[26] Zhao J L, Wang X H, Sun T Y and Li L T 2005 *Nanotechnology* **16** 2450
[27] Li T, Yang S G, Huang L S, Gu B X and Du Y W 2005 *Nanotechnology* **15** 1479
[28] Nielsch K, Muller F, Li A P and Gösele U 2000 *Adv. Mater.* **12** 582
[29] Liang Y Q, Zhai L, Zhao X S and Xu D S 2005 *J. Phys. Chem.* B **109** 7120
[30] Li L, Zhang Y, Li G H and Zhang L D 2003 *Chem. Phys. Lett.* **378** 244
[31] Harris G B 1952 *Phil. Mag.* **43** 113
[32] Barret C and Massalaski T B 1980 *Structure of Metals* (Oxford: Pergamon) p 204
[33] Tian M L, Wang J G, Snyder J, Kurtz J, Liu Y, Schiffer P, Mallouk T E and Chan M H W 2003 *Appl. Phys. Lett.* **83** 1620
[34] Dai Z R, Pan Z W and Wang Z L 2002 *J. Phys. Chem.* B **106** 902
[35] Cornelius T W, Brötz J, Chtanko N, Dobrev D, Miehe G, Neumann R and Toimil Molares M E 2005 *Nanotechnology* **16** S246
[36] Pan H, Liu B, Yi J, Poh C, Lim S, Ding J, Feng Y, Huan C H A and Lin J 2005 *J. Phys. Chem.* B **109** 3094
[37] Martín-González M, Prieto A L, Gronsky R, Sands T and Stacy A M 2002 *J. Electrochem. Soc.* **149** C546
[38] Weast R C, Lide D R, Astle M J and Beyer W H 1989 *Handbook of Chemistry and Physics* (Boca Raton, FL: CRC Press)

[39] Sauer G, Brehm G, Schneider S, Nielsch K, Wehrspohn R B, Choi J, Hofmeister H and Gösele U 2002 *J. Appl. Phys.* **91** 3243
[40] Sun M, Zangari G, Shamsuzzoha M and Metzger R M 2001 *Appl. Phys. Lett.* **78** 2964
[41] Wang X F, Zhang J, Shi H Z, Wang Y W, Meng G W, Peng X S and Zhang L D 2001 *J. Appl. Phys.* **89** 3847
[42] Das V D and Soundarajan N 1988 *Phys. Rev.* B **37** 4552
[43] Mansfield R and William W 1958 *Proc. Phys. Soc. London* **72** 733
[44] Augustine S and Mathai E 2003 *Semicond. Sci. Technol.* **18** 745
[45] Dheepa J, Sathyamoorthy R, Velumani S, Subbarayan A, Natarajan K and Sebastian P J 2004 *Sol. Energy Mater. Sol. Cells* **81** 305
[46] Singh M P and Bhandari C M 2003 *Solid State Commun.* **127** 649
[47] Lin Y M, Cronin S B, Ying J Y, Dresselhauls M S and Heremans J P 2000 *Appl. Phys. Lett.* **76** 3944
[48] Hicks L D and Dresselhaus M S 1993 *Phys. Rev.* B **47** 16631